

# Charge exchange in gas-surface collisions: Momentum transfer

John A. Olson and Barbara J. Garrison

*Department of Chemistry, Pennsylvania State University, University Park, Pennsylvania 16802*

(Received 16 September 1985; accepted 2 December 1985)

A description of near-resonant charge exchange in gas-surface collisions that includes momentum transfer is presented. The surface is represented by a cluster of metal atoms. A diatomics in molecules procedure is used to obtain the surface eigenvalues and eigenfunctions. These are combined with those of the gas atom or ion to construct the interaction potentials and electronic coupling terms. These provide the input needed to solve for the nuclear and electronic motions in the common eikonal formalism which leads to a time dependent description of the event. The formalism is applied to a sodium atom scattering from a W(110) surface. The surface consists of five W atoms. The center W atom is allowed to move during the collision. Transition probabilities are presented for various two and three electronic state systems and compared to the case where the position of the center W atom remains fixed.

## I. INTRODUCTION

In the experiments by Overbosch and Los,<sup>1</sup> a hyperthermal (30–400 eV) beam of alkali atoms was scattered from a tungsten (110) surface. Since the ionization potential of the alkali atom lies close to the work function of the metal, one would expect that transfers of an electron between the atom and surface should occur. Indeed, the experimental results indicated that most of the incoming neutral atoms were ionized by the surface.

Due to the close proximity of the alkali ionization potential and the tungsten work function, the mechanism for this type of electron transfer has been termed near-resonant charge exchange.<sup>2</sup> From a theoretical point of view, the electron transfer results from a breakdown of the Born-Oppenheimer approximation (i.e., there are couplings between electronic states due to nuclear motions). As a result, more than one electronic state is needed for the description of the system. In the adiabatic representation, the transitions between these states are caused by the nonadiabatic coupling terms (electronic matrix elements of the nuclear gradient operator). An alternative and often more useful representation is the diabatic electronic representation<sup>3</sup> where the transitions arise from the off-diagonal matrix elements of the electronic Hamiltonian.

A number of treatments for the multistate problem that use a classical description of the nuclear motions have been developed for gas phase collisions. Our interest has been involved in developing a theoretical description of near-resonant charge exchange occurring in hyperthermal energy collisions of an atom with a surface. The solution of the electronic problem is based on using a small cluster of atoms to represent the surface. A complete discussion of using such a description is found in Ref. 4. Standard electronic techniques result in well-defined interaction potentials and nonadiabatic couplings which are used in the semiclassical common eikonal formalism<sup>5</sup> (see Sec. II) to obtain the final state of the system. Electron transfer probabilities for a number of two<sup>4,6</sup> and three<sup>7</sup> electronic state systems have been calculated for a sodium atom scattering off a W(110) surface. The results showed an overall increase in the electron transfer probability with increasing kinetic energy of the sodium

atom. There was also an interesting oscillatory behavior of the probability for all cases studied.

In this paper, a study of the electron transfer probability is presented that takes into consideration the transfer of momentum of the sodium atom to the surface. In Sec. II the formalism on which our model is based is briefly reviewed. The electron transfer probability for some two and three electronic state systems is presented and discussed in Sec. III and compared to the case where momentum transfer does not occur. The paper ends with a conclusion in Sec. IV.

## II. THEORY

In this section a brief review of the formalism used to obtain the transition probabilities is presented. As was mentioned in the introduction, the common eikonal method requires the construction of the interaction potentials and nonadiabatic couplings. If an electronic basis consisting of the continuum states of the surface and the atomic states of the incident atom is used, the potentials and couplings resulting from this description become rather arbitrary due to the great difficulty in calculating them from first principles. In order to circumvent these problems, a small cluster of metal atoms is used to represent the surface. This representation of the surface leads to interaction potentials and nonadiabatic couplings that come from electronic procedures that are based on first principles.

A five atom cluster with geometry corresponding to the (110) face is used to represent the surface. The neutral surface has five electrons, one electron per surface atom, and the ionic surface has an additional electron on one of the cluster atoms. A formal treatment of the electronic problem for the neutral and ionic case that employs a simplified version of the diatomics in molecule procedure<sup>8</sup> is given in Ref. 9. This procedure is system dependent since it depends on the component diatomics. It leads to fifteen eigenvalues and eigenfunctions for the surface, five of which are neutral and ten ionic. The diatomic potentials needed in this approach and the eigenvalues obtained from it are given in Ref. 4. These eigenvalues and eigenfunctions are combined with the corresponding sodium eigenvalues and eigenfunctions (assuming one valence 3s electron on the sodium atom) in the polyato-

mics in molecule scheme<sup>10</sup> to obtain the sodium surface interaction potentials and nonadiabatic coupling terms. The diatomic potentials and the method used to construct the basis functions are also given in Ref. 4. This procedure results in fifteen interaction potentials, five of which are asymptotically neutral and ten asymptotically ionic. In Ref. 4 these potentials are shown for the case that the sodium atom approaches perpendicular to the surface and collides with the center tungsten atom. This choice of trajectory maintains the  $C_{2v}$  symmetry of the surface which reduces the number of states that couple.

In our previous treatments of this system, the positions of the surface atoms were held fixed, which resulted in a one-dimensional problem. In the present case of momentum transfer, the center tungsten atom is allowed to move during the collision. Letting  $R_w$  and  $R$  be the perpendicular position of the center tungsten atom and the sodium atom, respectively, relative to the plane of the surface, the nuclear kinetic energy operator is

$$\hat{T}_{nu} = -\frac{\hbar^2}{2m} \frac{\partial^2}{\partial R^2} - \frac{\hbar^2}{2m_w} \frac{\partial^2}{\partial R_w^2}, \quad (1)$$

where  $m$  and  $m_w$  are the masses of the sodium and tungsten, respectively. The center tungsten atom is held to the surface by a harmonic oscillator potential of the form

$$V_{ho} = \kappa R_w^2, \quad (2)$$

where  $\kappa$  is proportional to the force constant. The transition amplitudes satisfy the time-independent Schrödinger equation

$$(\hat{T}_{nu} + V^d + V_{ho})\Phi = E\Phi, \quad (3)$$

where  $V^d$  is the  $(n \times n)$  matrix representation of the electronic Hamiltonian in the diabatic basis and  $\Phi = \Phi(R, R_w)$  is the  $(n \times 1)$  column matrix of the nuclear wave functions. In the common eikonal treatment the solutions of Eq. (3) are written in the form

$$\Phi = \chi e^{i(\hbar)S}, \quad (4)$$

where  $S(R, R_w)$  is the eikonal which is common for all electronic channels. Using Eq. (4) in Eq. (3), defining

$$\frac{1}{2m} \left( \frac{\partial S}{\partial R} \right)^2 + \frac{1}{2m_w} \left( \frac{\partial S}{\partial R_w} \right)^2 + V = E, \quad (5)$$

and neglecting the second derivative terms<sup>4</sup> of  $\chi$  results in a first order differential equation for the  $\chi_i$  with

$$V = \chi^\dagger V^d \chi + V_{ho}, \quad (6)$$

where  $\chi^\dagger \chi = 1$  (see Ref. 4 for a complete analysis). Transforming into time [ $P(t) = \partial S(t)/\partial R$ , etc.; i.e., a momentum] leads to

$$\frac{\hbar}{i} \frac{dC}{dt} + V^d C = 0, \quad (7)$$

where  $C$  is the complex  $(n \times 1)$  column vector of the time dependent nuclear amplitudes. Equation (5) now becomes

$$\frac{P^2}{2m} + \frac{P_w^2}{2m_w} + V = E, \quad (8)$$

which is in the form of the Hamilton-Jacobi equation with

$$V = C^\dagger V^d C + V_{ho}. \quad (9)$$

Defining the Hamiltonian as

$$H(R, R_w, C) = \frac{P^2}{2m} + \frac{P_w^2}{2m_w} + V(R, R_w, C), \quad (10)$$

and letting

$$C_j = \frac{1}{\sqrt{2\hbar}} (C_j' + iC_j''), \quad (11)$$

gives

$$\frac{dC_j'}{dt} = -\frac{\partial H}{\partial C_j''}, \quad (12)$$

and

$$\frac{dC_j''}{dt} = \frac{\partial H}{\partial C_j'}, \quad (13)$$

which are in the form of Hamilton's equations of motion. The trajectories  $R(t)$  and  $R_w(t)$  are as yet unspecified. A convenient way of choosing these trajectories as well as  $P(t)$  and  $P_w(t)$ , which results in conservation of the total energy, i.e.,  $dH/dt = 0$ , is to require that

$$\frac{dR}{dt} = \frac{\partial H}{\partial P} = \frac{P}{m}, \quad (14)$$

$$\frac{dP}{dt} = -\frac{\partial H}{\partial R} = -\frac{\partial}{\partial R} (C^\dagger V^d C), \quad (15)$$

$$\frac{dR_w}{dt} = \frac{\partial H}{\partial P_w} = \frac{P_w}{2m_w}, \quad (16)$$

and

$$\frac{dP_w}{dt} = -\frac{\partial H}{\partial R_w} = -\frac{\partial}{\partial R_w} (C^\dagger V^d C) - 2\kappa R_w. \quad (17)$$

Equations (12)–(17) form a coupled set of first-order differential equations in time that self-consistently determine the real and imaginary parts of the electronic amplitudes as well as the nuclear "positions" and "momenta." The positions and momenta can not be strictly interpreted as the classical position and momenta because they depend on an average potential.

As is seen in Eq. (3), the common eikonal treatment is formulated in the diabatic electronic representation. Since the electronic problem is solved in the adiabatic representation, a transformation to the diabatic representation must be made. In the following, the dependence of the nonadiabatic coupling terms on  $R_w$  is neglected, i.e.,

$$d_{ij}^a(R_w) = \left\langle \Psi_i^a \left| \frac{\partial}{\partial R_w} \right| \Psi_j^a \right\rangle = 0, \quad (18)$$

where the  $\Psi_i^a$ 's are the adiabatic eigenfunctions and  $\langle \dots | \dots \rangle$  indicates an integration over electronic coordinates only. This assumption allows one to considerably simplify the calculation. The numerical accuracy of this assumption is discussed in the next section. In this case the diabatic eigenfunctions satisfy

$$\frac{\partial}{\partial R} |\Psi^d\rangle = 0, \quad (19)$$

where the superscript  $d$  denotes the diabatic representation. The two representations are related by a unitary transformation  $A(\Psi^d = \Psi^a A)$  so that Eq. (19) becomes

$$\frac{\partial A}{\partial R} + \left\langle \Psi^a \left| \frac{\partial}{\partial R} \right| \Psi^a \right\rangle A = 0, \quad (20)$$

which is a first-order differential equation for  $A(R, R_0)$  with the boundary condition that  $A(R_0, R_0) = 1$ .

Results for various two and three electronic state systems are presented in the next section. The transformation matrix for both these cases have been given by Top and Baer<sup>11</sup> (see also Ref. 7). With these transformations the diabatic potential energy matrix is given by

$$V^d = A^\dagger V^a A, \quad (21)$$

where  $V^a$  is the diagonal matrix of the adiabatic eigenvalues.

### III. RESULTS AND DISCUSSION

A typical calculation is done by numerically integrating Eqs. (12)–(17) using a standard integration procedure.<sup>12</sup> The center tungsten atom is initially at the origin ( $R_w = 0$ ) and at rest ( $P_w = 0$ ). The initial electronic state of the system is always the neutral channel. The probability of being in the electronic state  $j$  is

$$P_j = \frac{1}{2\hbar} (C_j^2 + C_j^p). \quad (22)$$

Further details for the calculation are found in Ref. 4. The integration is continued until the probabilities have stabilized after the collision.

The approximation introduced in Eq. (18) assumes that the couplings do not depend on the displacement of the center tungsten atom relative to the origin. In order to determine the reasonableness of this assumption, electronic calculations were done over a range of perpendicular displacements of the center tungsten atom. The calculations showed that the eigenfunctions remained unchanged. The eigenvalues varied but they all decreased by nearly the same amount as the value of  $R_w$  decreased. The sodium surface interaction potentials for the various positions of  $R_w$  were similar in shape to the  $R_w = 0$  case, but were displaced in energy somewhat due to the change of the surface eigenvalues. Since the eigenvalues (neutral and ionic) varied in a uniform manner, the gas-surface interaction potentials relative to each other showed little change in the coupling region. Thus, the positions and magnitudes of the nonadiabatic couplings were practically identical to the  $R_w = 0$  case. Therefore, the approximation of Eq. (18) should have a minor effect on the results.

In these calculations, the couplings are modeled with Gaussians. This simplifies the calculations considerably and at the same time keeps the essential physics. The parameters used in the Gaussians can be found in Refs. 4 and 7. The value of the constant  $\kappa$  used in the harmonic oscillator potential of Eq. (2) is  $9.86 \text{ eV/\AA}^2$ . This value was determined from a sum of pair potentials for an equivalent tungsten atom on the (110) face of a 30 atom tungsten crystal. The crystal consisted of two layers. The pair potentials of Ref. 13 were used which have the form of a Morse potential.

The energy transfer during the collision is approximately 40% over the entire range of kinetic energy. This corresponds to the energy transfer in a head-on elastic collision between two particles with masses of the sodium and tung-

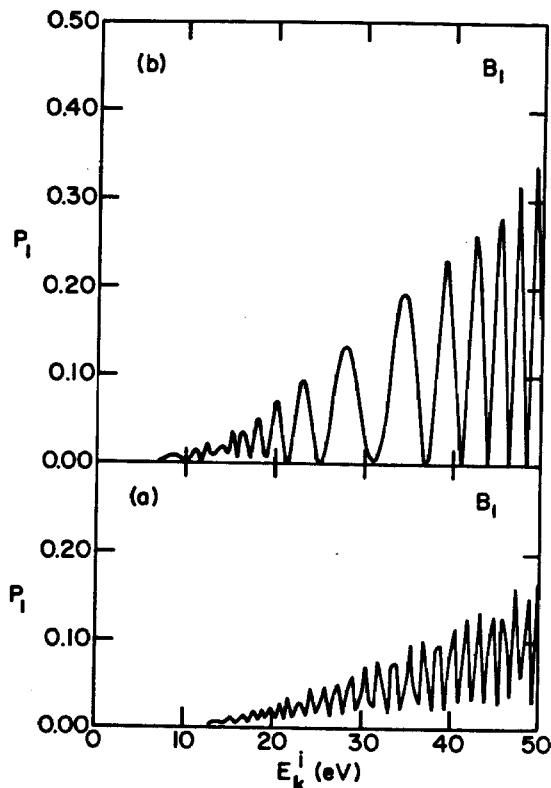


FIG. 1. Final values of the ionization probability,  $P_i$  vs the initial kinetic energy of the sodium atom for the  $B_1$  system: (a) with momentum transfer; (b) without momentum transfer.

sten atoms. Deviations from this do occur at the lowest energies (less than 10 eV) where the effect of the attractive well is more important.

#### A. Two electronic state systems

There are three states, one neutral and two ionic, that belong to the  $B_1$  irreducible representation of  $C_{2v}$  symmetry. However, only two of these effectively couple.<sup>4</sup> This system therefore reduces to a two electronic state system. The potentials and couplings for this system can be found in Ref. 4.

The electron transfer probability  $P_i$  versus the initial kinetic energy for the case of momentum transfer is shown in Fig. 1(a). The corresponding results for the case of no momentum transfer are shown in Fig. 1(b). A comparison of these cases shows a substantial decrease in  $P_i$  when momentum transfer occurs. This is not surprising since with momentum transfer the velocity of the sodium is less on its outward path than on its inward path. At lower velocities, the system tends to stay on the lowest adiabatic potential so that the outward path contributes on the average less to the electron transfer probability. Other comparisons worth noting are that the oscillations of  $P_i$  in Fig. 1(a) are more rapid and the minimum values of  $P_i$  are noticeably greater than zero (20–50 eV). The rate of oscillation depends on a phase that is proportional to a time integral of the difference of the two diabatic potentials. Even though the eigenvalues and eigenfunctions for the surface are the same for both cases, the interaction potentials are different due to the dependence for the case of momentum transfer on  $R_w$ . Therefore, a difference in the rate of oscillation is to be expected. That the oscillations in Fig. 1(a) do not go through zero is again a

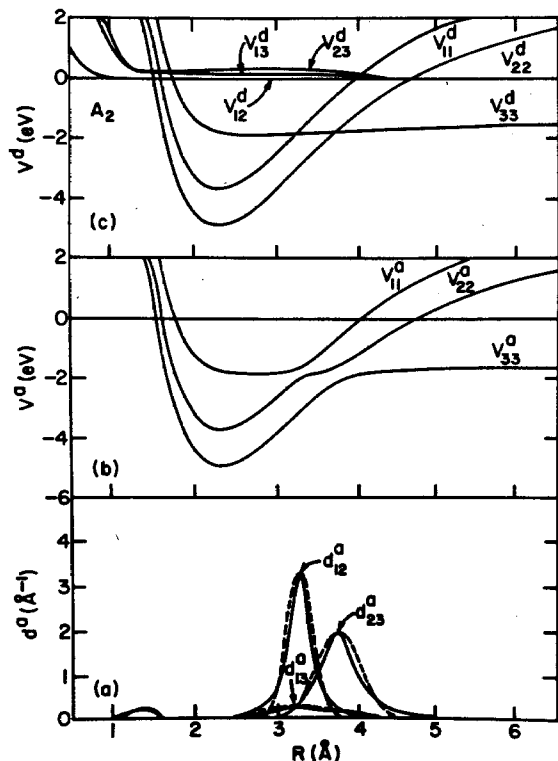


FIG. 2. Potentials and couplings of the  $A_2$  system for  $R_w = 0$ : (a) nonadiabatic couplings; (b) adiabatic potentials; (c) diabatic potentials.

consequence of the decrease in velocity on the outward path. If the transition probabilities were the same for the crossings on the inward and outward paths, one would expect that destructive interference would lead to a total cancellation, i.e.,  $P_1 = 0$ . However, since the velocities on the paths are different, which gives different transition probabilities, there should be only a partial cancellation so that  $P_1$  does not go through zero.

Another example of a two state system is given by the diabatic potentials  $V_{11}^d$  and  $V_{33}^d$  of the  $A_2$  states. Previous

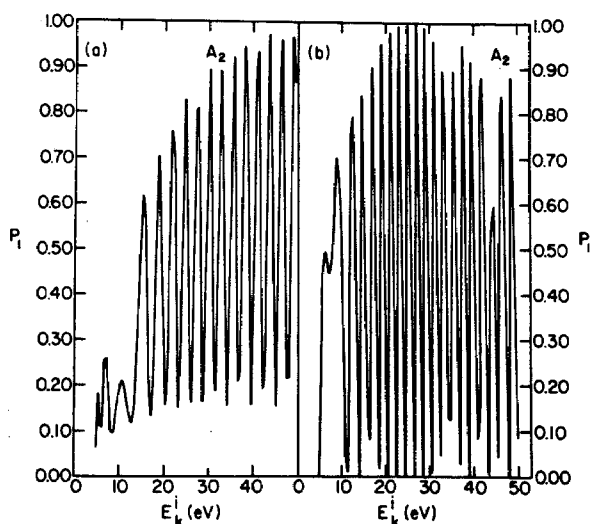


FIG. 3. Final values of the ionization probability  $P_1$  vs the initial kinetic energy for the two state  $A_2$  system: (a) with momentum transfer; (b) without momentum transfer.

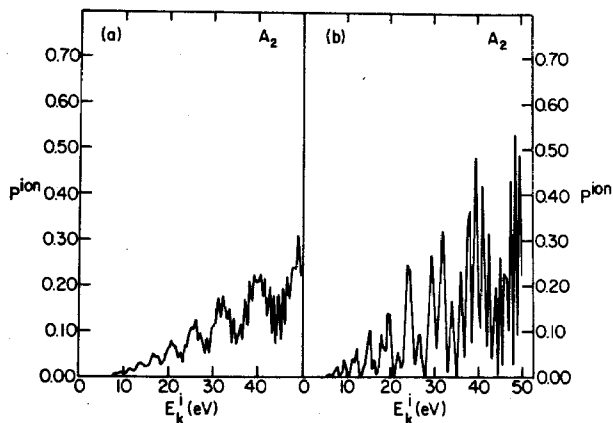


FIG. 4. Final values of the ionization probability  $P^{\text{ion}}$  vs the initial kinetic energy for the three state  $A_2$  system: (a) with momentum transfer; (b) without momentum transfer.

studies of this system showed a large tendency to transfer an electron. The potentials corresponding to  $R_w = 0$  are shown in Fig. 2(c) and the nonadiabatic coupling, designated as  $d_{12}^a$ , is shown in Fig. 2(a).

The results for the electron transfer probability with and without momentum transfer are shown in Figs. 3(a) and 3(b), respectively. One notices the same general trends as in the  $B_1$  case. However, since the probabilities without momentum transfer attain values close to unity at rather low energies ( $\approx 15$  eV), the decrease due to momentum transfer is not as noticeable as in the  $B_1$  case.

## B. Three electronic state systems

The states of  $A_2$  symmetry classification provide an example of a three electronic state system. The adiabatic and diabatic potentials are shown for  $R_w = 0$  in Figs. 2(b) and 2(c), respectively, and the nonadiabatic couplings for  $R_w = 0$  are shown in Fig. 2(a). The coupling between the ionic states,  $d_{13}^a$ , is small. In the following,  $P_1$  and  $P_2$  are the probabilities for being in the ionic states corresponding to  $V_{11}^d$  and  $V_{22}^d$ , respectively, and  $P_3$  is the probability of being in the neutral state corresponding to  $V_{33}^d$ .

The ionization probability  $P^{\text{ion}}$  with momentum transfer is shown as a function of the initial kinetic energy in Fig. 4(a).  $P^{\text{ion}}$  is defined as the sum of the probabilities for emerging in each ionic channel, i.e.,  $P_1 + P_2$ . The results with no momentum transfer are given in Fig. 4(b). As in the two state case, including momentum transfer leads to on the average a noticeable reduction in  $P^{\text{ion}}$ . This is due, as in the two state case, to the more adiabatic behavior on the outward path. Although not shown here, the contribution to  $P^{\text{ion}}$  by  $P_1$  is substantially less than that of  $P_2$ . This is in line with previous studies done without momentum transfer<sup>7</sup> which showed that most of the probability change occurred at the outer crossing. These previous studies also showed that the rapid oscillations characteristic of the two state case were superimposed on much slower oscillations [Fig. 4(b)]. These slower oscillations are due to the topological similarity of the two ionic potentials.<sup>7</sup> The difference in traveling the two ionic potentials varies much more slowly with energy than the corresponding neutral ionic case. Therefore, the

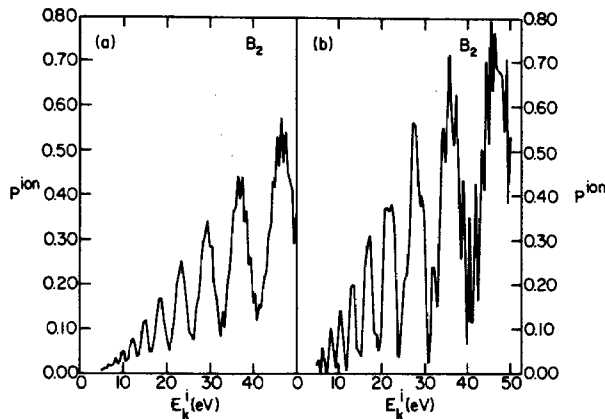


FIG. 5. Final values of the ionization probability  $P^{\text{ion}}$  vs the initial kinetic energy for the three state  $B_2$  system: (a) with momentum transfer; (b) without momentum transfer.

phase varies less rapidly with the initial energy which gives rise to the slower oscillations. The rapid oscillations in Fig. 4(b) are considerably damped in Fig. 4(a) and the reason for this was discussed in the two state section.

A final example is provided by the states belonging to the  $B_2$  symmetry classification. The potentials and couplings are similar to the  $A_2$  system and are therefore not shown here (see Ref. 7).

The results for  $P^{\text{ion}}$  with momentum transfer are shown in Fig. 5(a) and without momentum transfer in Fig. 5(b). A previous study<sup>7</sup> of this system [Fig. 5(b)] showed a rather large ionization probability so that the reduction caused by momentum transfer is not as great. The rapid oscillations that are superimposed on the slower ones in Fig. 5(b) are almost entirely damped in Fig. 5(a). The rate of the slower oscillations does not appreciably change with momentum transfer since it produces little relative change in the ionic potentials.

#### IV. CONCLUSION

The results presented here clearly demonstrate that momentum transfer can play a significant role in the electron

transfer probability. The major consequences of including momentum transfer is an overall decrease in the electron transfer probability and a noticeable change in its oscillatory behavior. The reason for this is simply due to a decrease in the velocity on the outward part of the trajectory. As a result, the transition probabilities on the inward and outward paths are not the same. Thus, on the average the probability for electron transfer is decreased. This change in probability on the outward path also results in less that total cancellation for destructive interference so that the ionization probability does not oscillate through zero. Since the electron transfer probabilities decrease in a fairly systematic way, this tends to support the idea that the outward path is more important in determining the average probability for electron transfer. As a final note, the oscillations seen here are simply a consequence of having more than one electronic channel available for the incoming sodium atom to emerge in, and it would be interesting to see if they could be experimentally detected.

#### ACKNOWLEDGMENTS

The financial support of the Office of Naval Research, the National Science Foundation, the IBM Corporation and the Camille and Henry Dreyfus Foundation is gratefully acknowledged.

- <sup>1</sup>E. G. Overbosch, R. Rasser, A. D. Tanner, and J. Los, *Surf. Sci.* **92**, 310 (1980).
- <sup>2</sup>J. C. Tully, *Phys. Rev. B* **16**, 4324 (1977).
- <sup>3</sup>F. T. Smith, *Phys. Rev.* **179**, 111 (1969).
- <sup>4</sup>J. A. Olson and B. J. Garrison, *J. Chem. Phys.* **83**, 1392 (1985).
- <sup>5</sup>D. A. Micha, *J. Chem. Phys.* **78**, 7138 (1983).
- <sup>6</sup>J. A. Olson and B. J. Garrison, *Nucl. Instrum. Methods* (in press).
- <sup>7</sup>J. A. Olson and B. J. Garrison (in preparation).
- <sup>8</sup>F. O. Ellison, *J. Am. Chem. Soc.* **85**, 3540 (1963).
- <sup>9</sup>J. A. Olson and B. J. Garrison, *J. Chem. Phys.* **81**, 1355 (1984).
- <sup>10</sup>J. C. Tully, in *Potential Energy Surfaces*, edited by K. P. Lawley (Wiley, New York, 1980).
- <sup>11</sup>Z. H. Top and M. Baer, *J. Chem. Phys.* **66**, 1363 (1977).
- <sup>12</sup>L. F. Shampine and M. K. Gordon, *Computer Solution of Ordinary Differential Equations: The Initial Value Problem* (Freeman, San Francisco, 1975).
- <sup>13</sup>L. A. Girifalco and V. G. Weizer, *Phys. Rev.* **114**, 687 (1959).